

Magnetic Fields in Supernova Remnants

John R. Dickel^A and D. K. Milne^B

^A University of Illinois Observatory, Urbana, Illinois 61801, U.S.A.

^B Division of Radiophysics, CSIRO, P.O. Box 76, Epping, N.S.W. 2121.

Abstract

Parkes 2.7 and 5.0 GHz polarization maps have been combined to obtain distributions of magnetic field, Faraday rotation and depolarization for 20 supernova remnants.

1. Introduction

The existence of significant magnetic fields in supernova remnants (SNRs) has been known since the identification of their radio continuum emission as synchrotron radiation. Because this emission is polarized (with the electric vector perpendicular to the magnetic fields within the source) the directions of the fields can be explored by polarimetric observations. However, a paucity of data has allowed little conclusive analysis. The few results which have been published indicate that the very young remnants have radially oriented magnetic fields (e.g. Cas A; see Mayer and Hollinger 1968) and the very old ones have more peripherally directed fields (e.g. 1209–51/52; see Whiteoak and Gardner 1968), but there have been insufficient data to show an evolutionary trend.

To provide information based on a resolution of 8'.4 arc for a reasonable sample of SNRs, we have undertaken a series of polarimetric observations at 2.7 GHz (Milne 1971*a*, 1971*b*, 1972; Milne and Dickel 1971, 1974) and 5 GHz (Milne and Dickel 1975) for a total of 20 remnants. Supplementary data are available at other frequencies for some of these sources. In Section 3 below we present maps of the distribution of magnetic field orientation, Faraday rotation and depolarization ratio for the 20 sources.

2. Procedure

The data at both 2.7 and 5 GHz were obtained with the 64 m telescope at Parkes, and the reader is referred to the observational papers (Milne 1972; Milne and Dickel 1974, 1975) for the original data and a discussion of their errors and other aspects. The first step in the comparison of the data at the two frequencies was to convolve the 5 GHz maps (HPBW 4'.4 arc) to the 8'.4 arc resolution of the 2.7 GHz maps. The 2.7 GHz data were also interpolated to identical positional grids with the 5 GHz data so that direct point-by-point analysis was possible. This finer grid spacing also helps the reader to visualize the structure better; however, it must be borne in mind that the resolution is still only 8'.4 arc.

Multiple-frequency information is needed to evaluate and remove the effect of Faraday rotation by the free electrons and any longitudinal magnetic field between the source and the observer, whether internal or external to the SNR. This effect, caused by different indices of refraction for propagation of the ordinary and extraordinary modes in a magnetoionic medium, produces a net rotation of the electric vector given by the relation

$$PA(\text{observed}) - PA(\text{intrinsic}) + n(180^\circ) = K\lambda^2 \int_S^O N_e \mathbf{B} \cdot d\mathbf{l}, \quad (1)$$

where PA is the position angle of the \mathbf{E} vector measured in the usual fashion eastward from north; K is a constant; λ is the wavelength; the integration is between the source S and observer O , with N_e the electron density, \mathbf{B} the magnetic field strength and \mathbf{l} the path length through the medium; and n is an integer to account for the 180° ambiguity in measuring position angles. Thus measurements on at least three frequencies are necessary to solve unambiguously for the rotation and the intrinsic position angle of the polarized vector. In most cases, because only two-frequency data are available, we have assumed $n = 0$ unless evidence from nearby sources or continuity in field directions and rotation have indicated otherwise. Where multiple-frequency or independent evidence is available, this assumption has been generally confirmed. However, the results must still be treated with some caution as wrong conclusions can very easily be drawn from measurements at only two frequencies. This has been demonstrated most prominently in the case of 3C10 where, from observations over a relatively large λ^2 interval of from 10.4 to 21 cm, Weiler and Seielstad (1971) suggested an average rotation measure (RM) of $+37 \text{ rad m}^{-2}$, whilst using additional data at 2.8 and 6 cm Duin (1974) showed that the most likely RM was -242 rad m^{-2} .

For our observations, over the relatively short λ^2 baseline corresponding to 2.7–5 GHz, a change in n of $+1$ would produce a shift of $+74^\circ$ in intrinsic position angle and would decrease the rotation measure by 360 rad m^{-2} ; these values are sufficiently high to generally discriminate between $n = 0, 1, 2, \dots$. Offsetting this advantage of the short frequency baseline there is an increase in the random error in intrinsic position angle and rotation measure. From the probable errors in the measured position angles (typically $\pm 10^\circ$ and $\pm 5^\circ$ at 2.7 and 5 GHz respectively) the error in intrinsic position angle would be $\pm 9^\circ$ and in rotation measure about $\pm 23 \text{ rad m}^{-2}$; these are fairly moderate errors. Lastly it is possible for the rotation to be nonlinear with λ^2 , a situation that can arise if the Faraday rotation is within the emitting region; data at many different frequencies may be necessary to assess this effect.

(a) Magnetic Field Distributions

The intrinsic orientation of the projected electric vector of the synchrotron emission at each point on the source can be determined by the simultaneous solution of equation (1) at the two wavelengths considered. In (a) of Figs 1–20 we have plotted vectors whose directions are perpendicular to the intrinsic electric vectors and hence parallel to the projected magnetic field. The lengths of these vectors are proportional to the average of the polarized intensities at the two frequencies and are thus some measure of the degree of order of the fields and of our confidence in the

results. Also sketched are the total-intensity contours at 5 GHz to show the overall structure of the SNR. These contours are taken from Milne and Dickel (1975) and have a resolution of $4'.4$ arc.

(b) *Faraday Rotation*

The solution of equation (1) also gives the integral product of the electron density and the longitudinal magnetic field—generally termed the rotation measure. The actual integral is

$$\int_s^{\circ} N_e \mathbf{B} \cdot d\mathbf{l} = 1.23 \times 10^{-6} \times RM,$$

where N_e is in cm^{-3} , B in gauss (10^{-4} T), l in parsec and RM in rad m^{-2} .

In (b) of Figs 1–20 the rotation measure over each SNR is shown by symbols. The scale for the rotation measures represented by these symbols is defined by a specific RM value given in each figure. The positive values (net magnetic field directed toward the observer) are represented by filled symbols and negative values (field directed away) by open symbols. For 1209–51/52 (Fig. 4) the data were so sparse that the rotation measures are given next to the magnetic field vectors and not included in separate plots.

(c) *Depolarization*

The fractional polarization observed for each SNR generally averages less than 10%, which implies considerable twisting and tangling of the projected fields. In addition, there is generally a decrease in the polarization at lower frequencies which we have quantized by defining a ‘depolarization ratio’ as the percentage polarization at 5 GHz divided by that at 2.7 GHz. This ratio is displayed in (c) of Figs 1–20 only for points where the total power brightness temperatures on the original maps were greater than 0.04 K or about five times the r.m.s. noise level, i.e. only where meaningful percent polarizations on the sources were available. Symbols, similar to those in (b), are used to represent the depolarization, and the scale for these is given in Fig. 1c.

3. Results

Figs 1–20 show the derived maps of the magnetic fields, Faraday rotation measures and depolarizations. One would expect that the directions of the projected magnetic field and the distribution of rotation measure are much as we have shown in these figures unless extreme values for the rotation measures are envisaged. There remain, however, unexplained discontinuities in several of the rotation-measure maps (e.g. Puppis A, MSH 15–52 and Kesteven 27); their removal (by the addition of 180° rotation between 2.7 and 5 GHz) would only result in equally abrupt changes in the magnetic field directions.

Two sources, MSH 17–39 and Kepler’s SNR, are too small to be resolved in our observations. The present results for MSH 17–39 (Fig. 12) differ markedly from those of Kundu *et al.* (1974) and can be explained by our different treatment of the strong background polarization. The magnetic fields in a further seven of these sources have been discussed by various authors; brief notes on these are given below.

G188.9+3.0, IC 443 (Fig. 1). The general picture of the projected component of the magnetic field sweeping down from the north and curving off eastward is quite

evident across the middle of this source. One interpretation is that the field lines emanate near the southern peak, on the edge of a zone of high depolarization. This area of the remnant also contains a point source, which is unresolved on the aperture synthesis map constructed at Westerbork (Duin 1974) (and possibly has a flatter spectral index than the surrounding area; Colla *et al.* 1971), and the end of an apparent jet of neutral hydrogen (DeNoyer 1972), each or neither of which may be related to the SNR. The Faraday rotation appears smaller throughout the remnant than indicated by Kundu and Velusamy (1972) but our intrinsic position angles agree reasonably well. Fig. 1 could be obtained with a higher resolution ($4'.8$ arc) by comparing our 5 GHz data with the 2.7 GHz survey of Baker *et al.* (1973). An approximate comparison between these two sets of results showed only small differences from Fig. 1.

G296.5+9.7, 1209-51/52 (Fig. 4). The 2.7 GHz data for this source were taken from the paper by Whiteoak and Gardner (1968), who also used the Parkes instrument. Because the source is very extended, complete polarimetric maps are not available and the Faraday rotation has been determined only at the selected points shown in Fig. 4. The lines represent the orientation of the magnetic field and the adjacent values are the Faraday rotation in rad m^{-2} . In agreement with Whiteoak and Gardner, who analysed 1.4 and 2.7 GHz data, we find a tangential orientation of the magnetic field around the bright edges of the SNR. The Faraday rotation is always small and appears to have a moderate east-west gradient.

G326.2-1.7, MSH 15-56 (Fig. 8). The magnetic field pattern appears to be deflected around the bright south-western component of this source. We agree with Whiteoak and Gardner (1971) that the strongest polarization delineates a radial magnetic field but our more complete results show that this does not hold true over the more weakly polarized regions. The depolarization shows little correlation with the structure of the source but is generally very strong except on the western side.

G327.6+14.5, SNAD1006 (Fig. 10). This SNR shows the radially oriented magnetic field pattern typical of young remnants, e.g. Cas A (Mayer and Hollinger 1968; Downs and Thompson 1972) and the remnant of Tycho's supernova (Duin 1974). The low Faraday rotation in the directions of the brightest parts of the shell is a reflection of the low-surface brightness of this source and the consequently relatively high, randomly polarized, background noise at 5 GHz. The sharp contrast in depolarization between the south-western and north-eastern arcs is unexplained.

Figs 1-20 (pp. 439-58). Distributions over 20 SNRs of (a) direction of projected magnetic field (the vector length represents only the average 5 and 2.7 GHz polarization temperature and not necessarily the magnetic field strength), (b) Faraday rotation measure and (c) depolarization. Fig. 4 is an exception to this format, since the magnetic field direction and rotation measure were obtained at only a few positions in each remnant (see text). The data in each figure (except 4) are in a $2'$ arc grid with a resolution of $8'.4$ arc, while the superimposed contours of 5 GHz total power brightness temperature (K), from Milne and Dickel (1975), have a resolution of $4'.4$ arc. Galactic coordinates are shown for all maps.

In (b) of the figures, the value of the rotation measure RM at each point is represented by one of seven graduated symbols, filled for positive values of RM , open for negative values; the scale for each figure is defined by the specific RM value given.

In (c), similar symbols to (b) are used to specify the depolarization (always positive), with the addition of a cross to represent values less than unity; the common scale is given in Fig. 1c.

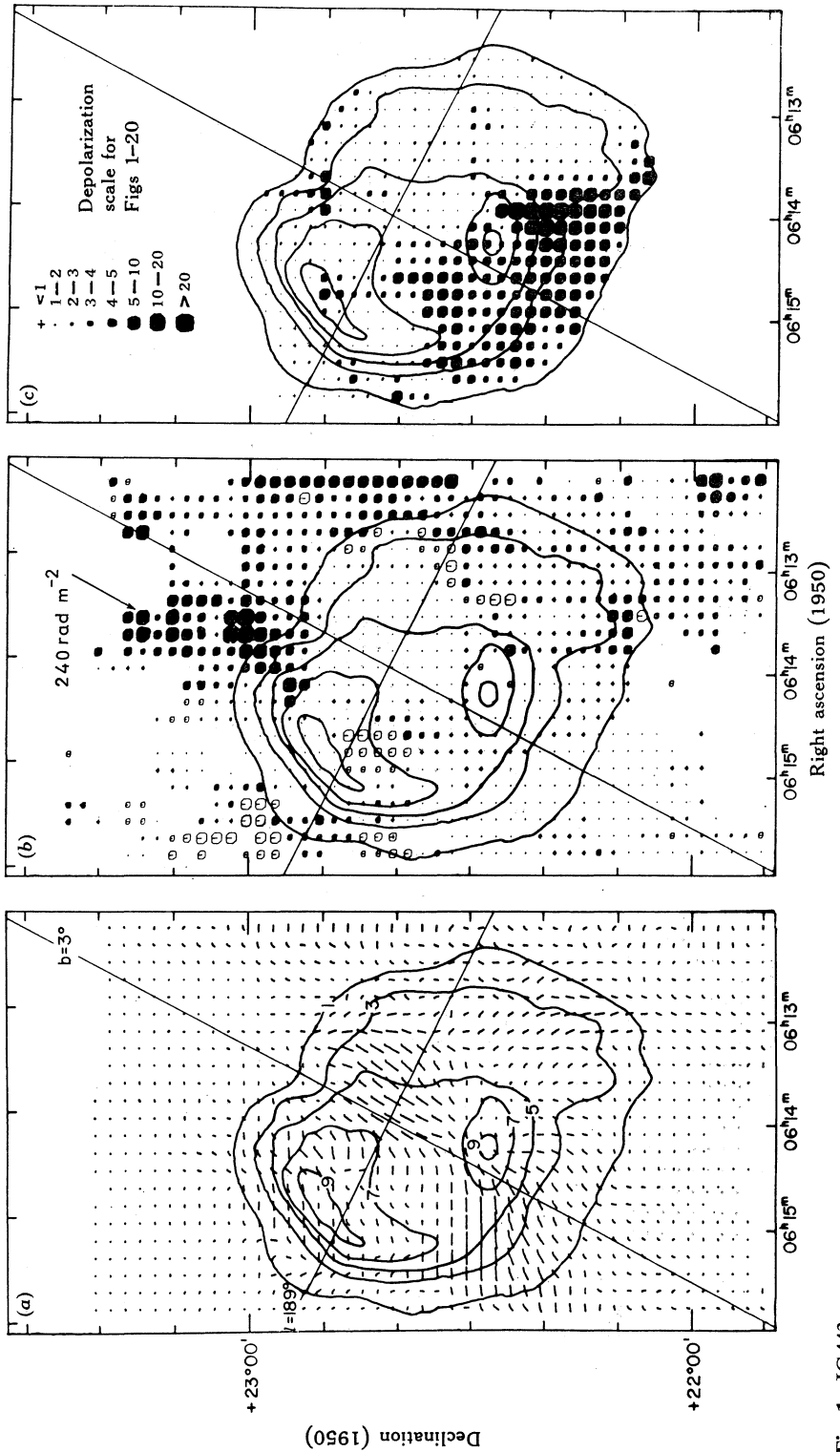


Fig. 1. IC443

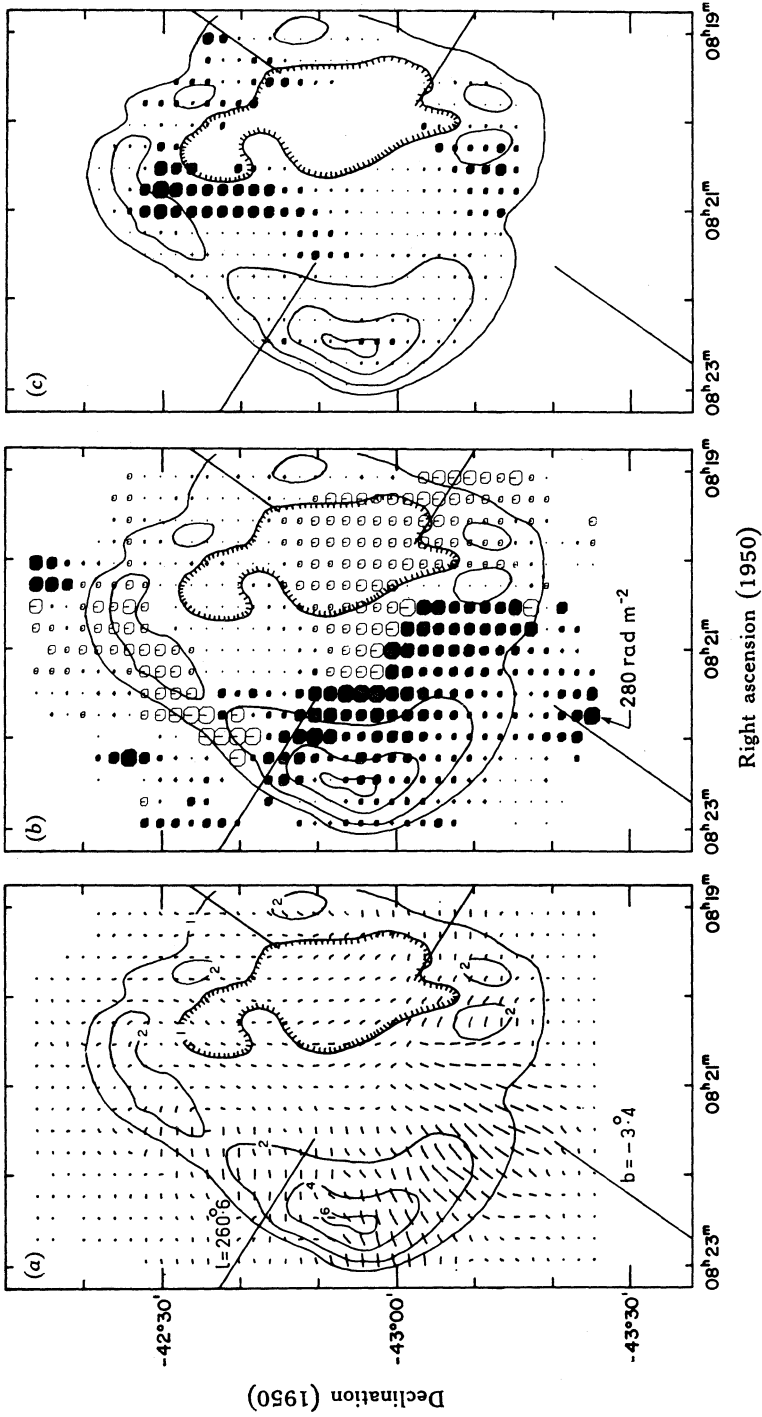


Fig. 2. Puppis A

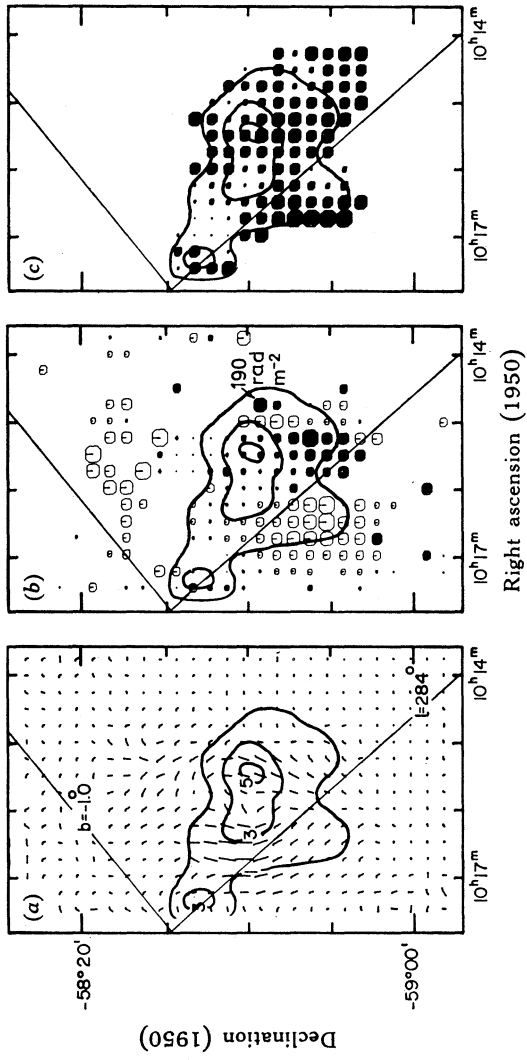


Fig. 3. MSH 10—53

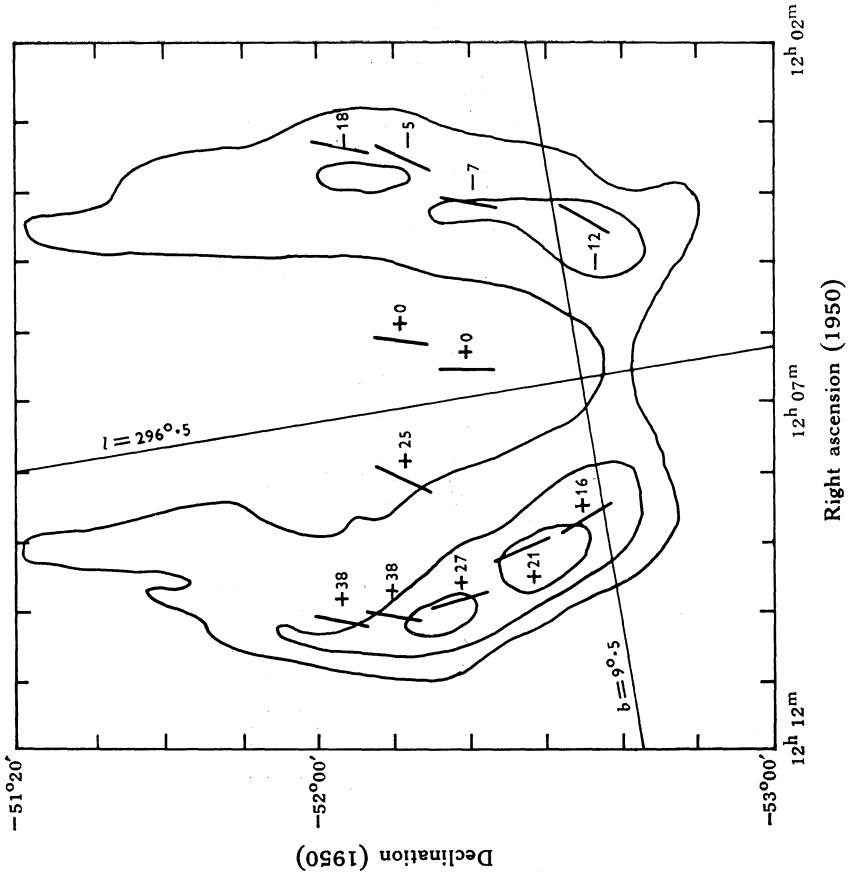


Fig. 4. 1209-51/52

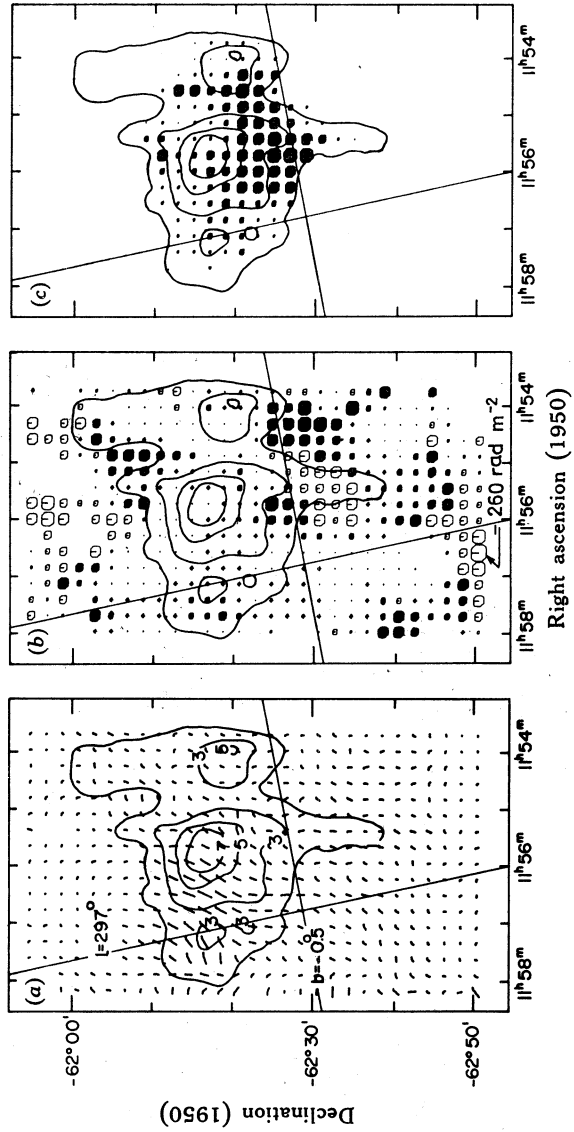


Fig. 5. 1156-62

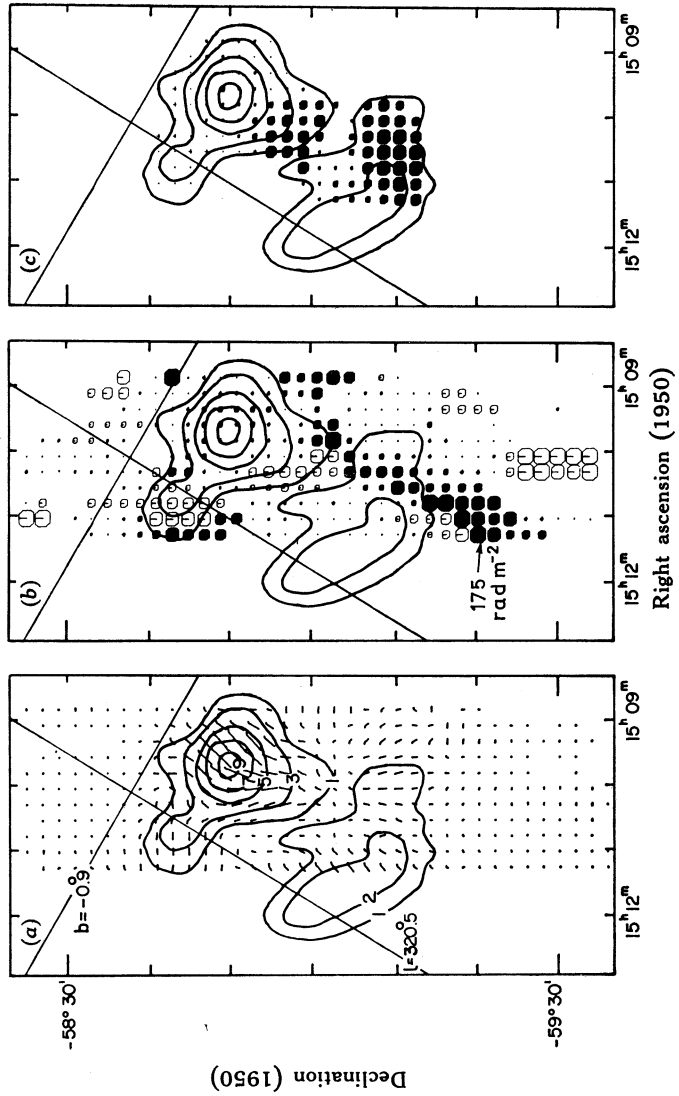


Fig. 7. MSH15-52

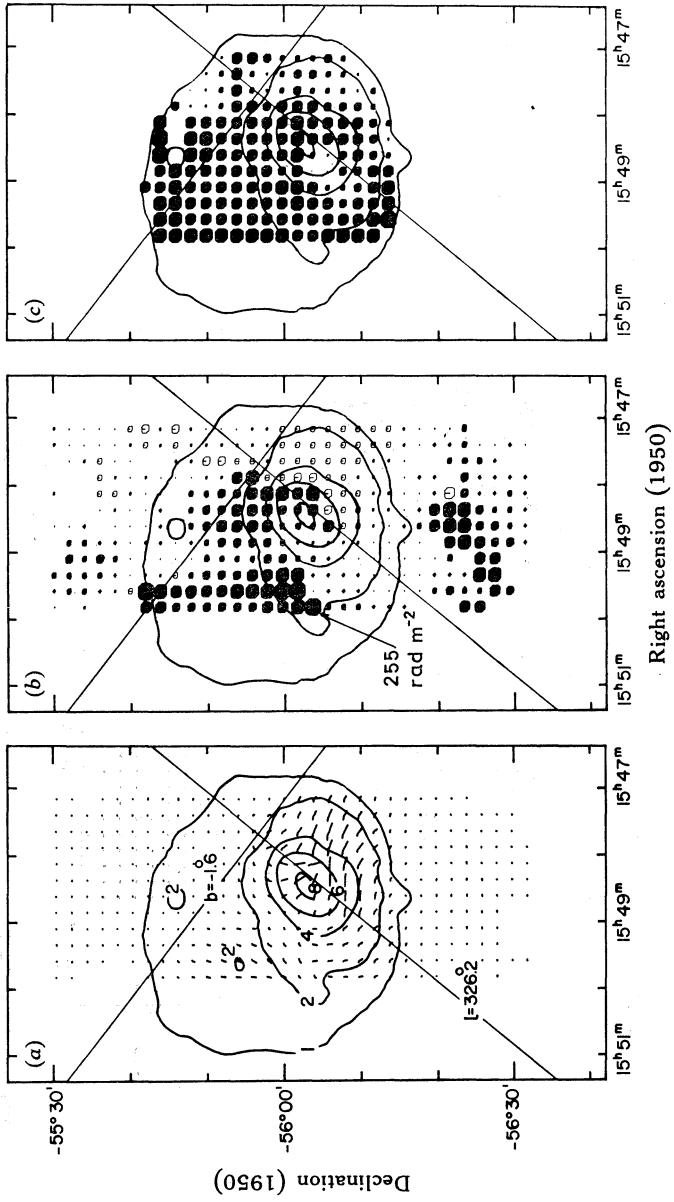


Fig. 8. MSH15-56

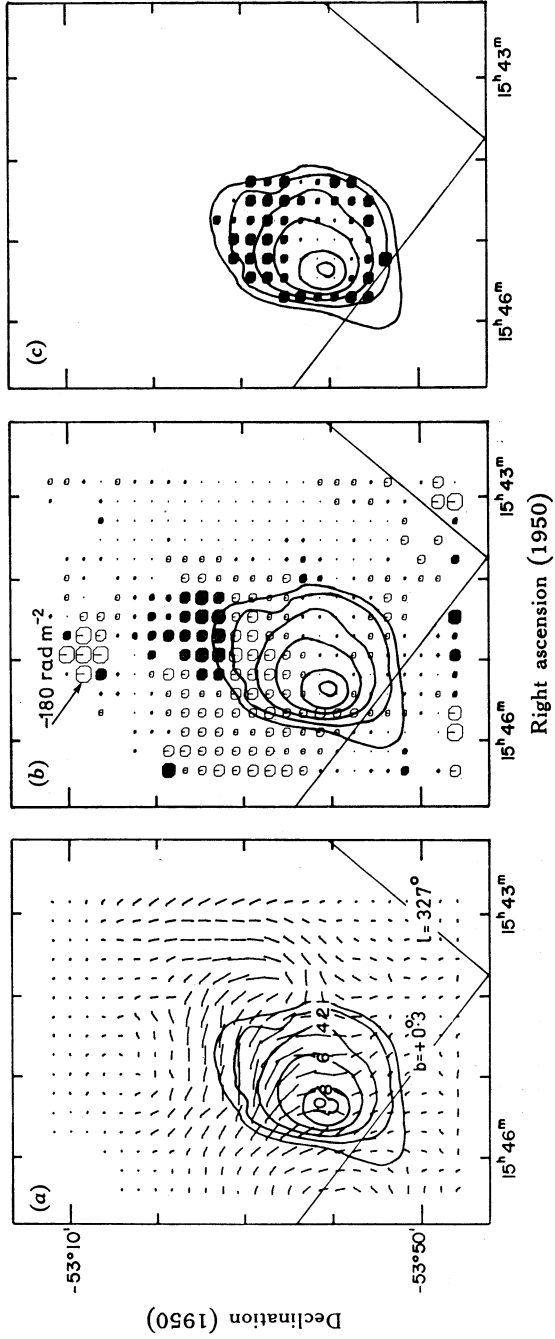


Fig. 9. Kesteven 27

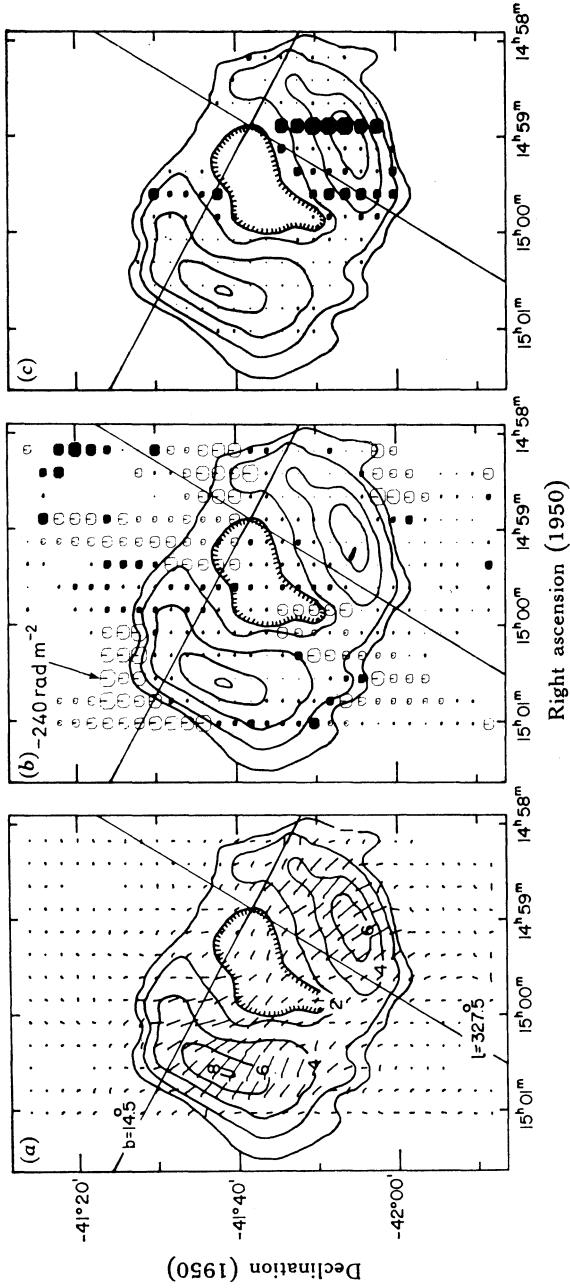


Fig. 10. SNAD1006

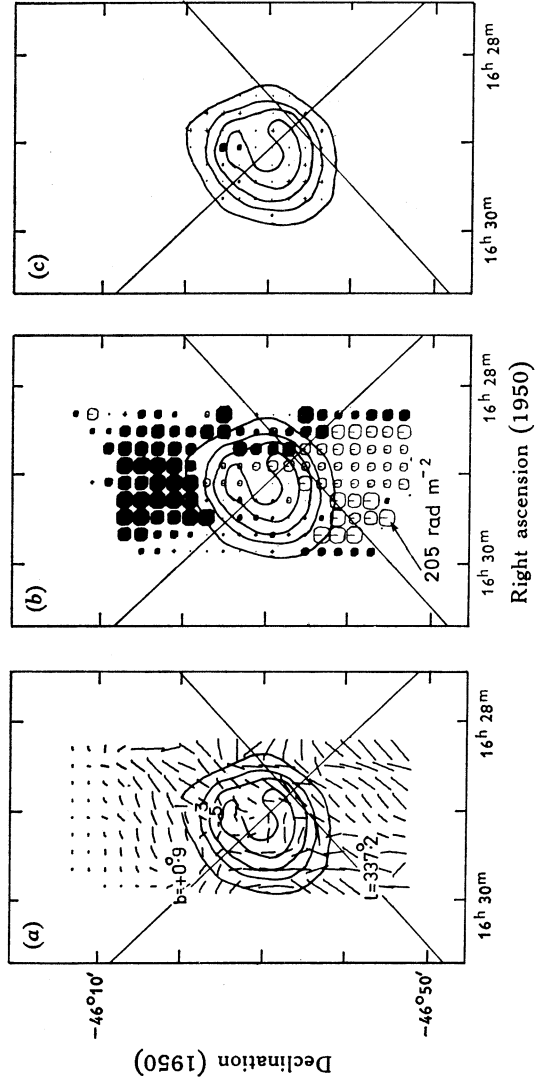


Fig. 11. Kesteven 40

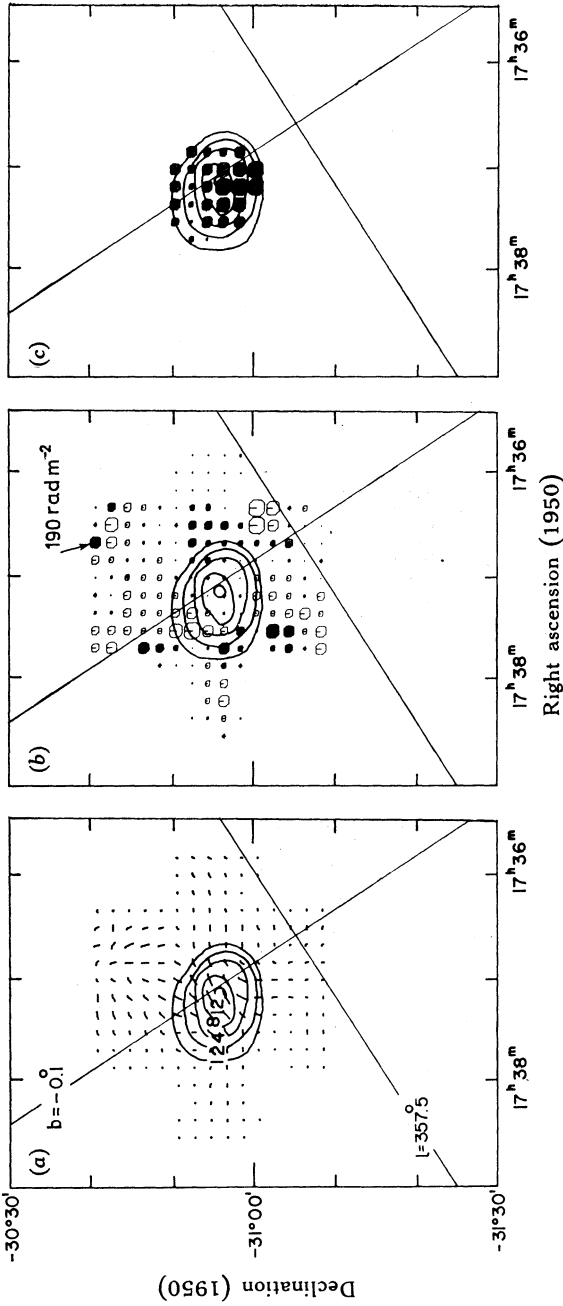
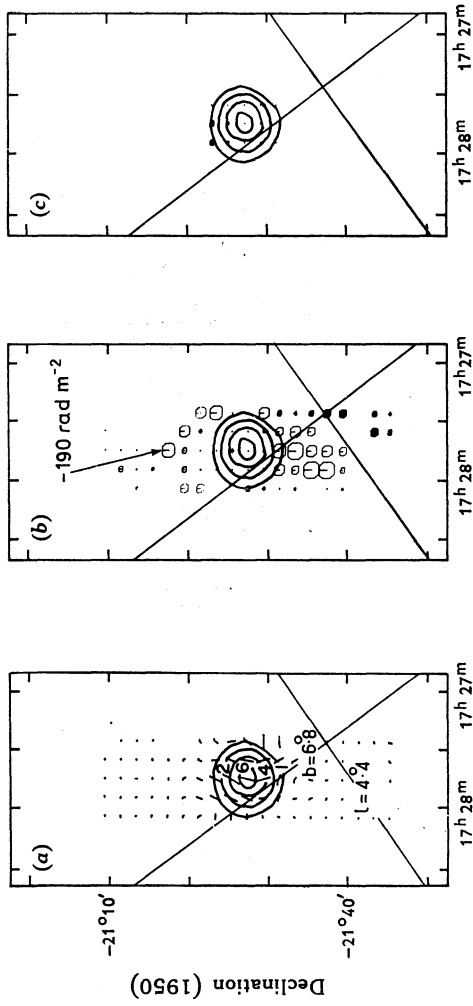
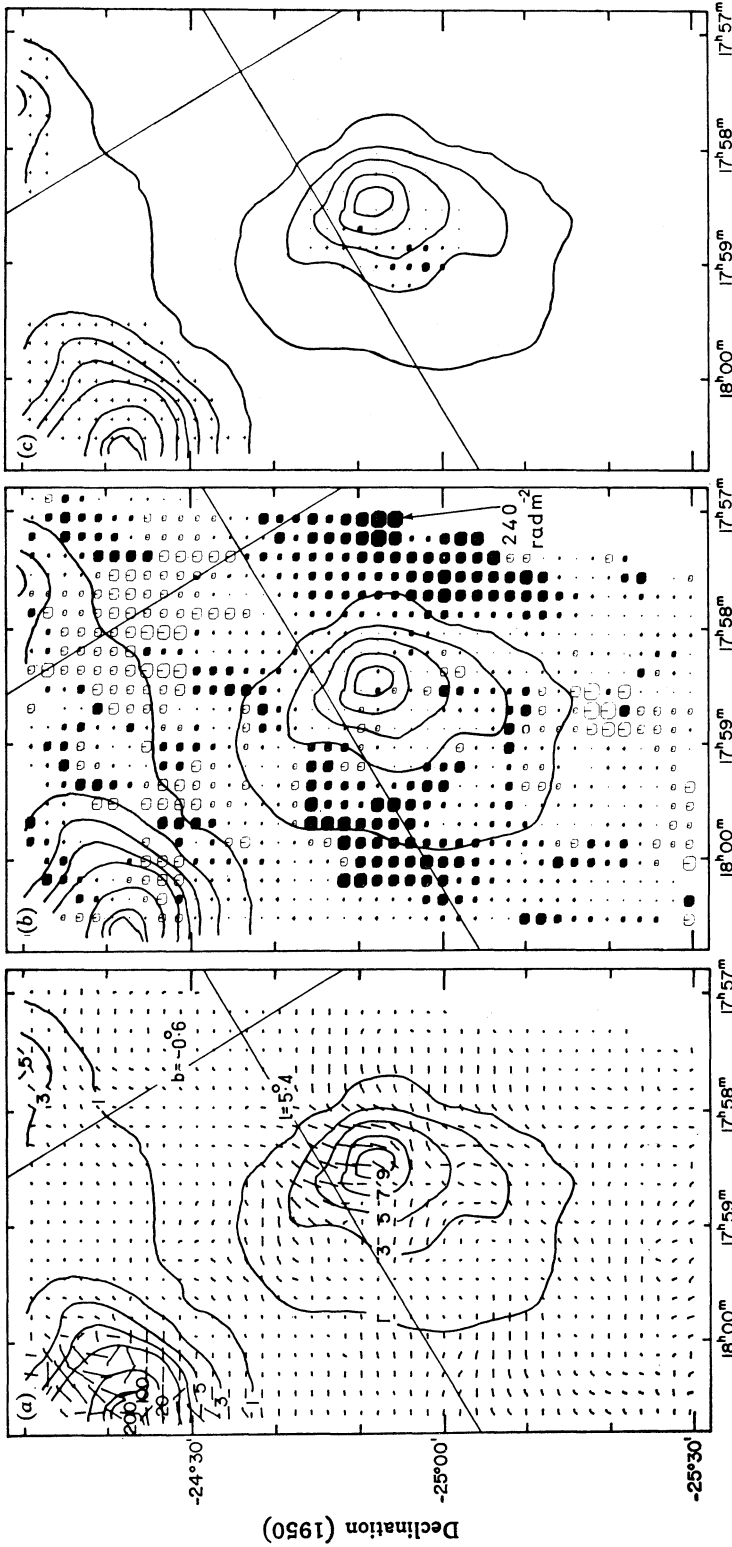


Fig. 12. MSH 17-39



Right ascension (1950)

Fig. 13. Kepler's SNR



Right ascension (1950)

Declination (1950)

Fig. 14. Milne 56

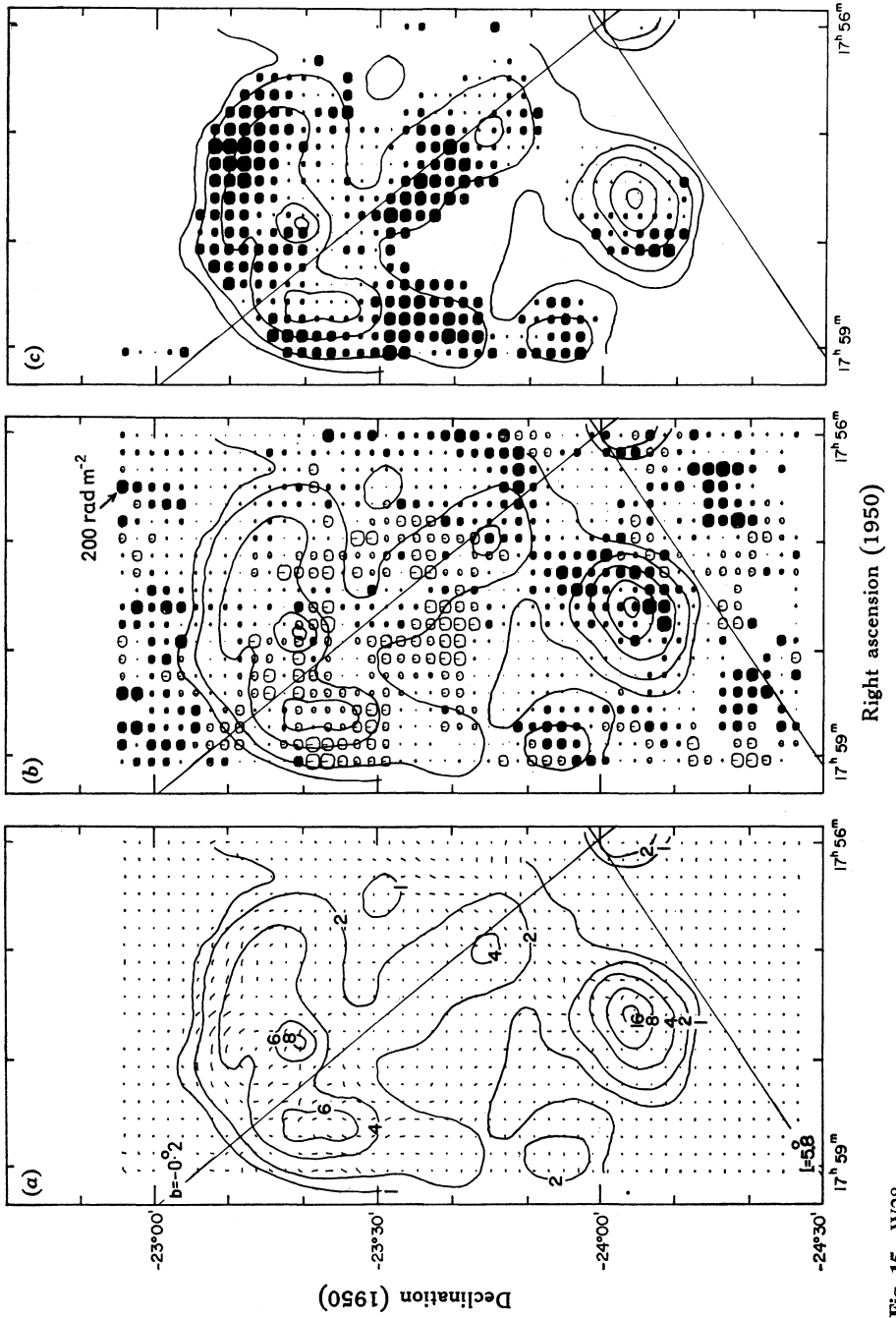


Fig. 15. W28

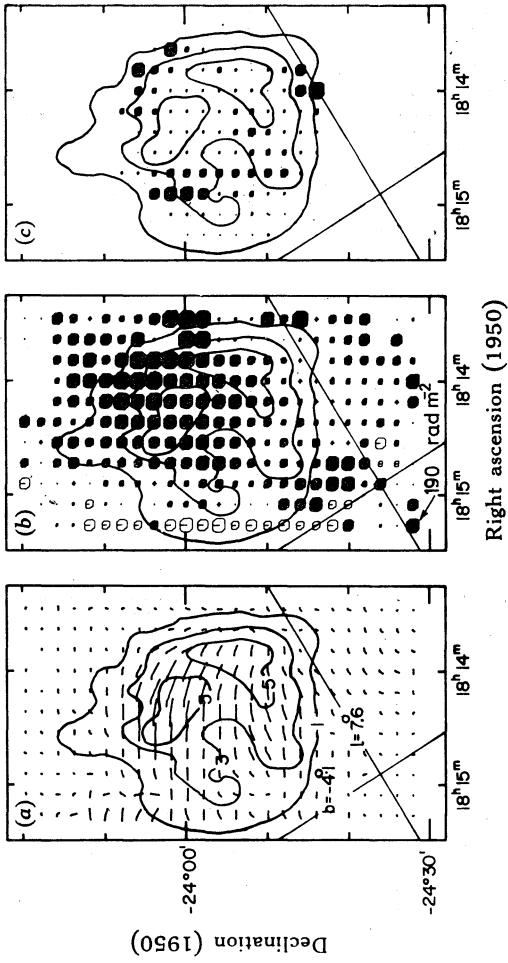


Fig. 16. 1814-24

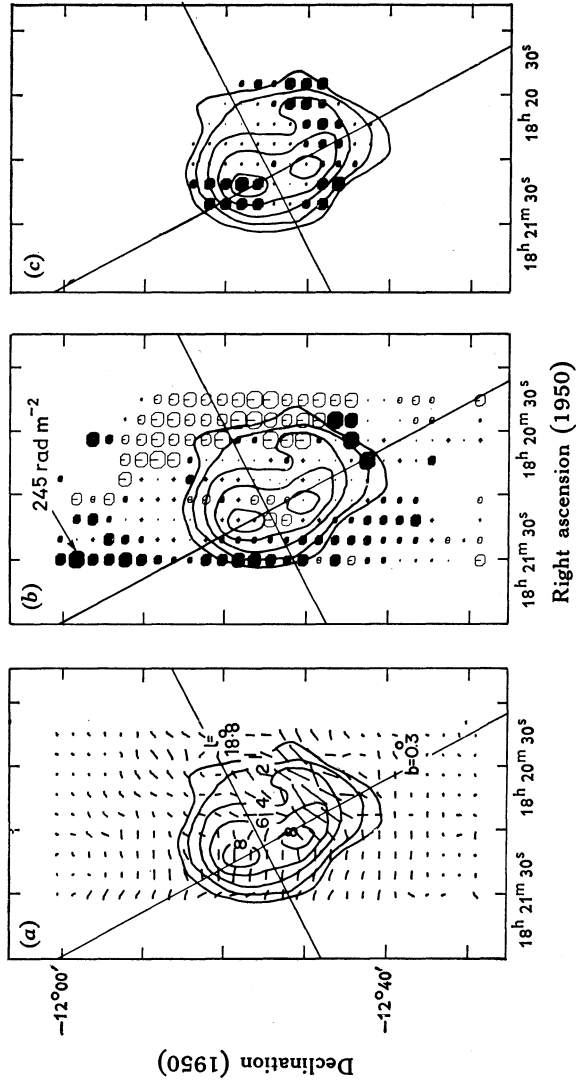
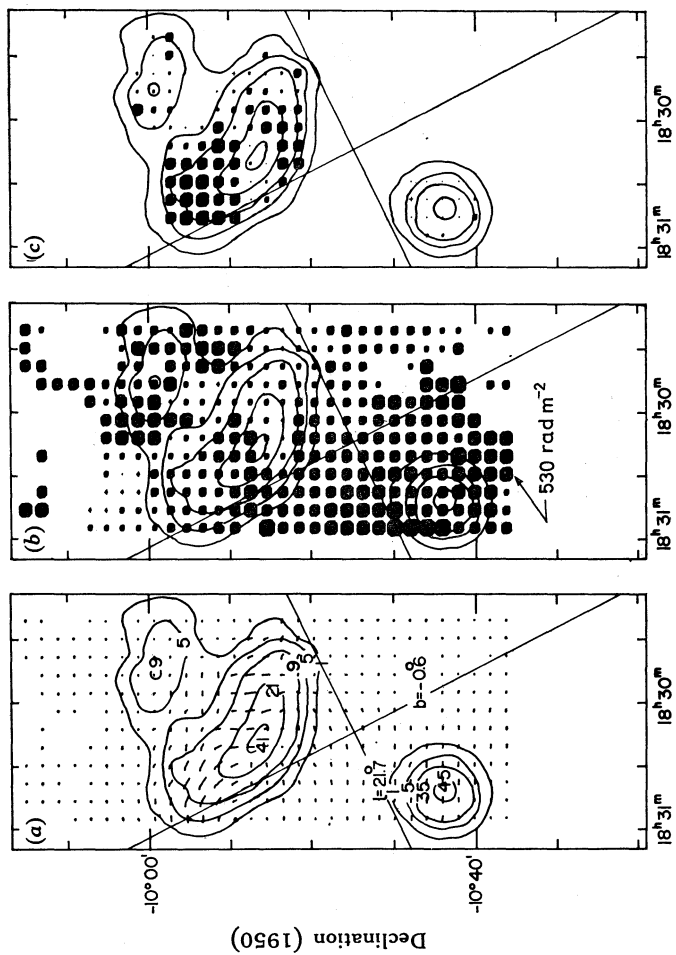


Fig. 17. Kesteven 67



Right ascension (1950)

Declination (1950)

Fig. 18. Kesteven 69

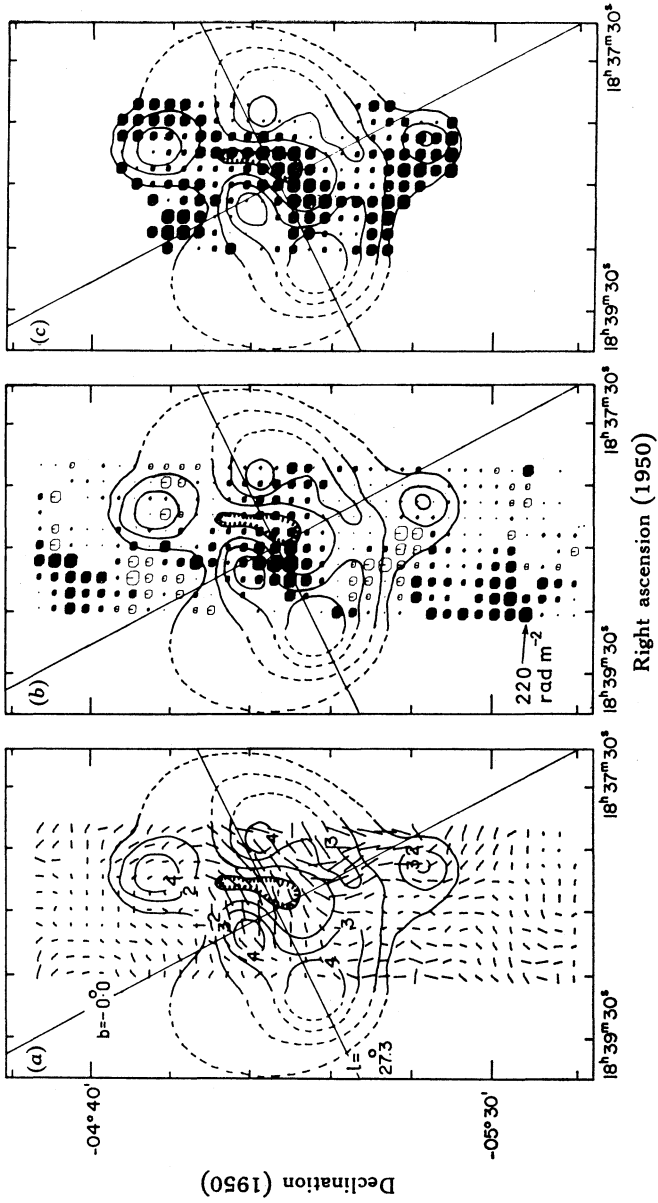


Fig. 19. Kesteven 73

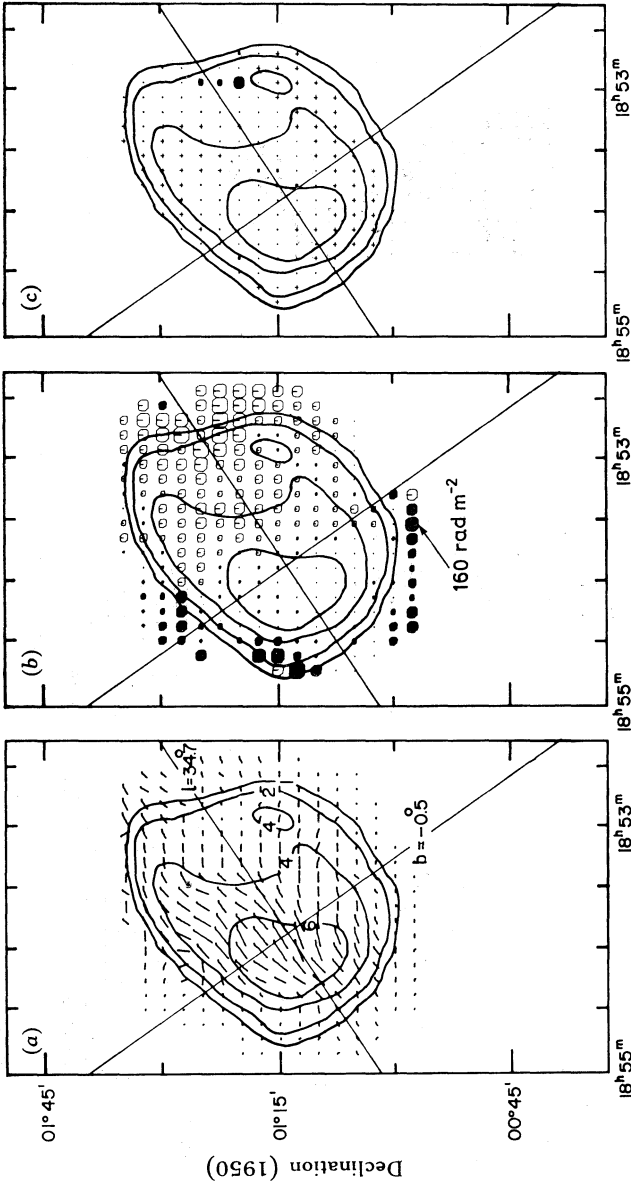


Fig. 20. W44

G6.6-0.2, W28 (Fig. 15). This is one of the few remnants that appears to have a circumferential magnetic field around the bright arc of the shell and the entire remnant appears to fall within one large reasonably smooth cell of negative Faraday rotation. The bright peak in the south-centre of this map is an HII region. Our magnetic field directions agree fairly well with those of Kundu and Velusamy (1972) (governed almost entirely by their 2.8 cm observations) but we disagree strongly with their rather extreme values for the Faraday rotation (dependent on their 6 and 2.8 cm data). The depolarization is relatively high over this source.

G21.8-0.6, Kesteven 69 (Fig. 18). Comparison of our data at 2.7 and 5 GHz with those of Kundu *et al.* (1974) at 10.6 GHz shows that the Faraday rotation is very large over most of the SNR and the differences between the position angles at 2.7 and 5 GHz shown in Fig. 18 are actually the measured values plus 180° . The extreme rotation measures off the source are artificial and are the result of inclusion of this extra 180° where it perhaps does not apply. The field appears to vary smoothly across the bright southern shell of the SNR changing from radial to tangential in different spots. The nature of the small-diameter source G21.9-0.7 to the south of Kesteven 69 is unknown.

G34.6-0.5, W44 (Fig. 20). Fig. 20 was constructed from the 5 GHz map of Whiteoak and Gardner (1971) and from our 2.7 GHz data. The polarization at both frequencies is strong and uniformly directed, leading to a fairly unambiguous magnetic field and a well-defined gradient in the rotation measure, both approximately orthogonal to the galactic equator. These results agree well with those of Kundu and Velusamy (1972) and Baker *et al.* (1973).

4. Discussion

Although the polarimetric parameters of the various remnants are very complex and often present a confusing picture, a few general conclusions emerge from the data.

(i) One effect is an apparent evolutionary separation of magnetic field patterns into two groups (possibly corresponding to the first and third evolutionary phases of an SNR discussed by Woltjer 1970).

- (1) The young SNRs, such as Cas A (Downs and Thompson 1972), 3C 10 (Duin 1974) and AD 1006 (present paper), clearly show radially oriented fields, implying a stretching of the field lines as the remnant rapidly expands.
- (2) Some of the very old remnants (1209-51/52 and W44)* show magnetic field patterns tangential to the brightest parts of the SNR shell, suggesting a possible compression of the surrounding field.

Several of the SNRs (like Kesteven 67) show rather different patterns in various positions across the remnant, possibly because of different evolution rates as various

* One must be careful in affixing an age to an SNR from its position on the Σ - D diagram. The determinations by Milne (1970) and the independent one by Downes (1971) are good computations demonstrating the trend of the evolution but they also illustrate the very statistical nature of the relation which no later attempts have been able to clarify. For example, the historical and morphological (and magnetic field) data for AD 1006 appear far more persuasive than the surface brightness, and we claim it is truly young. For W44, the 21 cm line measurements give a good estimate of the distance (3 kpc), which means it must have linear dimensions of 30 pc and must therefore be quite old. This would appear to be a firmer conclusion than the conclusion, based on the highly statistical surface-brightness versus diameter relation, that it is smaller.

parts of a remnant interact with clouds of different density in the surrounding medium. A single remnant of one chronological age may possess a range of evolutionary ages in different parts. Presumably these objects, the bulk of the SNRs treated here, are in Woltjer's (1970) second phase.

(ii) In all sources the mean degree of polarization is generally low (usually $<10\%$ at 5 GHz) so that most of the emitting region contains a tangled magnetic field of which we view only a small net portion. A few sources (such as IC 443 and Puppis A) show significantly reduced polarization on their total-intensity peaks, possibly because of either a longer path length through a large number of turbulent cells or greater tangling in regions of higher emissivity.

(iii) Generally neither the Faraday rotation nor the depolarization shows any correlation with the observed total intensity. Any alignment of the gradient in rotation measure either perpendicular or parallel to the galactic equator is probably only fortuitous.

It is not clear to what extent the SNR magnetic field is coupled to the general galactic field. We feel that there is an interaction and that the magnetic field strength is in fact stronger close by an SNR than elsewhere (e.g. Kesteven 27 and MSH 17–39). This hypothesis has not yet been tested but clearly large areas around SNRs should be mapped in polarization to gauge the full extent of the magnetic field.

Acknowledgments

We thank M. Borrelli, R. Holman, E. O'Donnell and A. VanHoozen for assistance with the analysis and Dr Linda DeNoyer for stimulating discussion and thoughtful comments. The research was supported in part by the U.S. National Science Foundation Grant No. GP41560 to the University of Illinois.

References

- Baker, J. R., Preuss, E., and Whiteoak, J. B. (1973). *Astrophys. Lett.* **14**, 123.
 Colla, G., *et al.* (1971). *Astron. J.* **76**, 953.
 DeNoyer, L. K. (1972). Ph.D. Thesis, Cornell University.
 Downes, D. (1971). *Astron. J.* **76**, 305.
 Downs, G. S., and Thompson, A. R. (1972). *Astron. J.* **77**, 120.
 Duin, R. M. (1974). Ph.D. Thesis, University of Leiden.
 Kundu, M. R., and Velusamy, T. (1972). *Astron. Astrophys.* **20**, 237.
 Kundu, M. R., Velusamy, T., and Hardee, P. E. (1974). *Astron. J.* **79**, 132.
 Mayer, C. H., and Hollinger, J. P. (1968). *Astrophys. J.* **151**, 53.
 Milne, D. K. (1970). *Aust. J. Phys.* **23**, 425.
 Milne, D. K. (1971a). *Aust. J. Phys.* **24**, 429.
 Milne, D. K. (1971b). *Aust. J. Phys.* **24**, 757.
 Milne, D. K. (1972). *Aust. J. Phys.* **25**, 307.
 Milne, D. K., and Dickel, J. R. (1971). *Nature* **231**, 33.
 Milne, D. K., and Dickel, J. R. (1974). *Aust. J. Phys.* **27**, 549.
 Milne, D. K., and Dickel, J. R. (1975). *Aust. J. Phys.* **28**, 209.
 Weiler, K. W., and Seielstad, G. A. (1971). *Astrophys. J.* **163**, 455.
 Whiteoak, J. B., and Gardner, F. F. (1968). *Astrophys. J.* **154**, 807.
 Whiteoak, J. B., and Gardner, F. F. (1971). *Aust. J. Phys.* **24**, 913.
 Woltjer, L. (1970). In 'Interstellar Gas Dynamics', IAU Symp. No. 39 (Ed. H. J. Habing), p. 229 (Reidel: Dordrecht, Holland).